Indian Journal of Pure & Applied Physics
Vol. 53, June 2015, pp. 399-403

Synthesis, crystal structure and magnetic studies of ZnY_2O_4 oxide

Bidhu Bhusan Das*, Venugopal Potu & Govinda Rao Ruppa

Functional Materials Chemistry Laboratory, Department of Chemistry,

Pondicherry University, Puducherry 605 014 (India)

*E-mail: das_b_b@yahoo.com, venupotu@gmail.com, govindchem2005@gmail.com

Received 7 April 2014; revised 17 December 2014; accepted 16 April 2015

ZnY_2O_4 oxide is prepared by sol-gel method via nitrate-citrate route. Powder X-ray diffraction (XRD) study shows orthorhombic unit cell with lattice parameters: a = 10.8290 Å, b = 7.4518 Å, c = 6.0985 Å, space group Pccn and Z=4. Average crystallite sizes determined by Scherrer relation are found to be ~26-59 nm showing the formation of nanopaticles in the oxide. On Rietveld refinement of the unit cell structure, the agreement factors are lowered to: R_p=97.02%, R_{wp}=95.91% and R_{exp}=0.23%. The selected bond lengths are: Y_2-O_1: 3.7389 Å, Y_1-O_2: 3.0492 Å, Y_2-O_3: 2.1847 Å and Zn-O_1: 1.4088 Å, Zn-O_2: 3.7035 Å, Zn-O_3: 2.2777 Å. Formation of hysteresis loop in the range from-7.0 kG to +7.0 kG indicates the soft ferromagnetic nature of ZnY_2O_4 at 300 K. Density functional theory (DFT) calculation shows the valence band (VB) is spread over the range ~-9.0 to 0.0 and comprises mainly of O 2p and Y 4p, 4d, 5s orbitals, and the conduction band (CB) in the range from ~0.0 to 3.0 eV and comprises mainly of Y 4s, 4p and 4d orbitals. Very low value of energy band gap ~0.011 eV indicates weak semiconducting nature of ZnY_2O_4.

Keywords: Sol-gel synthesis, Powder X-ray diffraction, Magnetic studies, Density functional theory calculations

1 Introduction

A solid endowed with useful properties becomes a material and tailoring specific properties in solids (electrical, magnetic, dielectric, etc.) in correlation with the structure[1,2] is important from the point of view of potential applications as a material. In this regard, single phase complex oxides, particularly containing transition metal ions in nanosize powder form represent an important class of materials. As by changing the concentration of constituents or by chemical manipulations one can change the particle size, shape, composition and structure, one can control to an extent the electronic, magnetic, optical and other important characteristics of the materials[3]. As the conventional solid-state route is inappropriate to synthesize nanosize material, as it results in coarsening of grains, inhomogeneity, imprecise control of cation stoichiometry etc., this method is, thus, getting supplemmented by several unconventional wet chemical methods like sol-gel, combustion, precursor, coprecipitation, reverse micelle and hydrothermal[4]. Out of these unconventional methods, sol-gel method has several advantages over other synthesis techniques in various ways, such as purity, homogeneity, ability to produce nanosize powder etc.[5]. Todays nanomaterials attract great research interest due to their potential applications in areas such as information storage media, electronic devices, sensors, medical diagnostics agents[6,7] etc. In the present paper, the sol-gel synthesis of ZnY_2O_4 powder, and studies on structure-property relations using varieties of techniques, and calculations of electronic properties using DFT, have been reported.

2 Experimental Details

The sample is prepared by sol-gel method. To the mixture of 0.1 M solution each of required amounts of $Zn(NO_3)_2$ and $Y(NO_3)_3$ in H_2O 30 ml, dilute HNO_3 is added and stirred for 90 h at ~ 45°C to form sol. To the sol 40 ml of 1.5 M citric acid is added and the pH of the sol is adjusted to 2.0 for smaller particle size[8]. The sol is dried by continuous stirring for 36 h at ~ 45°C to form gel. The gel is decomposed at ~ 100°C to powder which was then calcined at 450°C for 6 h followed by sintering at 850°C for 6 h, to obtain fine powder sample. Powder XRD pattern of the sample is recorded on a Philips powder X-Ray diffractometer (Model X'pertpro; Pan Analytical) with step size 0.02, scan rate 2°/min in the range 10°-80° in 2θ. Monochromatic CuK_α radiation (λ ~1.54056 Å) is used as the X-ray source with power 40 kV/30 mA. Scanning electron micrographs (SEM) are taken using HITACH-S3400 and Energy

Dispersive X-rays (EDX) is done by 'Super dryer-II' model analyzer. Differential thermal analysis (DTA)/ differential scanning calorimetry (DSC) and thermogravimetric analysis (TGA) data are recorded on a thermogravimetric analyser (TA instruments, Q600 SDT and Q20 DSC) in the range 25-1000°C. Optical absorption spectrum in the range 200-800 nm is recorded by using a UV-visible spectrophotometer (Shimadzu Model: 2450). Bulk density of the sample is determined by liquid displacement method using CCl_4 as the immersion liquid (density 1.596 g/cc at 300 K). Electronic energy band structures and density of states (DOS) are calculated using a plane-wave DFT theory with local gradient-corrected exchange-correlation functional[9] and performed with a commercial version of the CASTEP (Cambridge Serial Total Energy Package) programme package[10,11] using Material Studio (MS) software which uses a plane-wave basis set for the valence electrons and norm-conserving pseudopotential[12] for the core electrons.

3 Results and Discussion

3.1 Powder X-ray diffraction analysis

Figure 1 shows the powder XRD pattern of ZnY_2O_4 along with the indexed lattice planes. Using the Fullprof program package the unit cell type and the lattice parameters are determined. By comparing the value of the calculated density with that of the observed value the value of Z is determined to be 4. Unit cell parameters and the calculated and the observed densities of the sample are presented in Table 1. In spite of having the same compositional formula as that of a spinel oxide, $A^{+2}B_2^{+3}O_4^{-2}$ (Ref. 13), ZnY_2O_4 is a non-spinel oxide with orthorhombic unit cell. Average crystallite sizes determined by Scherrer relation[14] are found to be in the range ~26-59 nm which show the formation of nanoparticles in the sample.

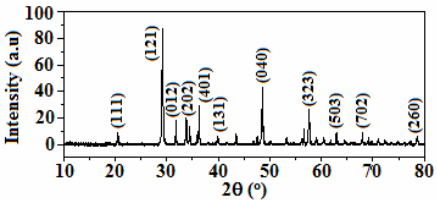

Fig. 1 — Unit cell parameters of ZnY_2O_4

3.2 SEM and EDX studies

SEM micrographs focussed at different points of the sample shows scattered nanorods [Fig. 2(a-b)]. EDX profile of the sample [Fig. 2(c)] shows the presence of elements O, Zn and Y in the sample in agreement with the composition. Mapping of all the constituent elements individually shows uniform distribution of the elements indicating the homogenity of the sample. Weight loss upto ~ 400°C with corresponding broad peak around 300°C in the DTA/DSC-TGA traces (Fig. 3) corresponds to physically and chemically adsorbed water in the sample. On further heating upto 1000°C, no significant event is observed in the sample.

3.3 Crystal structure refinement and Fourier electron density mapping

Unit cell structure of ZnY_2O_4 is developed on space group Pccn (IT No. 56) and Z = 4 with Y^{3+} ions in 4(a) and 4(c), Zn^{2+} ions in 4(c) and O^{2-} ions in 4(c),4(b) and 8(e) Wycoff positions. After Rietveld refinement[15] the agreement factors are lowered to: R_p = 97.02 %, R_{wp} = 95.91 %, and R_{exp} = 0.23 %. The

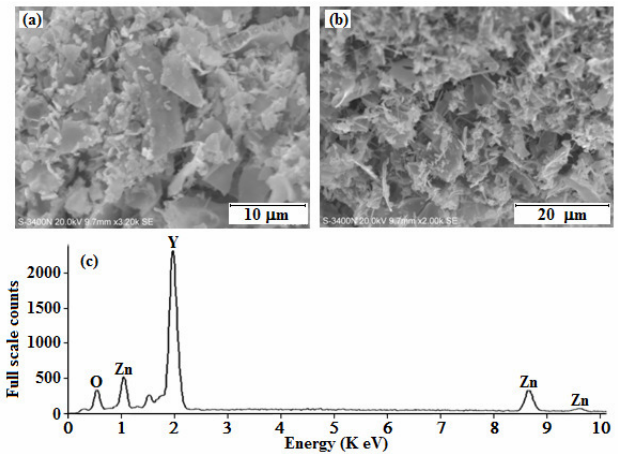

Fig. 2 — SEM micrographs of ZnY_2O_4: (a) 10 µm, (b) 20 µm at different magnifications, (c) EDX profile of ZnY_2O_4

Table 1 — Unit cell parameters, calculated and observed densities of ZnY_2O_4

Unit cell type	a* (Å)	b* (Å)	c* (Å)	Unit cell volume* (Å^3)	Observed density (g/cc)	Calculated density (g/cc)	Space group	Z
Orthorhombic *after refinement	10.8290	7.4518	6.0985	492.122	4.945	5.146	Pccn	4

refined unit cell dimensions are: a=10.8290 Å, b = 7.4518 Å, c = 6.0985 Å, and the calculated density, ρ_{cal}= 4.957 g/cm^3. The powder XRD pattern generated for ZnY_2O_4 from the developed unit cell structure is an idealized one, while the observed XRD pattern is from the nanosize powder of ZnY_2O_4 sample. These results are found to be in significant difference in widths of calculated and observed diffraction peaks, and as a result, larger values of the agreement factors are obtained. Perspective view of the unit cell structure of ZnY_2O_4 and projection onto (001) plane are shown in Fig. 4(a-b), while in Table 2 the crystal coordinates and the atomic coordinates before and after refinement are shown. The bond lengths are found to be: Y1-O2: 3.0492 Å, Y2-O1:3.7389 Å, Y2-O3: 2.1847 Å and Zn-O1: 1.4088 Å, Zn-O2:3.7035 Å and Zn-O3:2.2777 Å in the unit cell. It is important to mention that the spinel oxides ($A^{2+}B_2^{3+}O_4^{2-}$) are cubic with space group Fd-3mZ (IT 227) and Z=8 with ionic distribution in the unit cell as follows: A^{2+} in 8(a), B^{3+} in 16(d) and O^{2-}in 32(e) Wycoff sites[13], whereas, ZnY_2O_4 is a non-spinel oxide with orthorhombic unit cell. Such deviation from the spinel oxide structure of the $A^{2+}B_2^{3+}O_4^{2-}$ oxides are reported as in the cases of $MgAl_2O_4$ (Ref.16) and $CaMn_2O_4$ (Ref.17) oxides. From the comparison of the crystal radii[18] of the A^{2+} and B^{3+} cations in the cases of $A^{2+}B_2^{3+}O_4^{2-}$ spinels with the non-spinel oxides and the present oxide under study, we infer that rather than the relative values of the crystal radii of A^{2+} and B^{3+} cations, the synthetic condition is the dominant factor for the formation of the $A^{2+}B_2^{3+}O_4^{2-}$ spinel or non-spinel oxides. Fourier electron density mapping in 3-dimension from <001> plane and 2-dimensional electron density contour on (001) plane ZnY_2O_4 are shown in Fig. 4(c-d). The discontinuous but nearly circular contours around the ions indicate partial covalent character in the Y-O and Zn-O bonds in the unit cell structure.

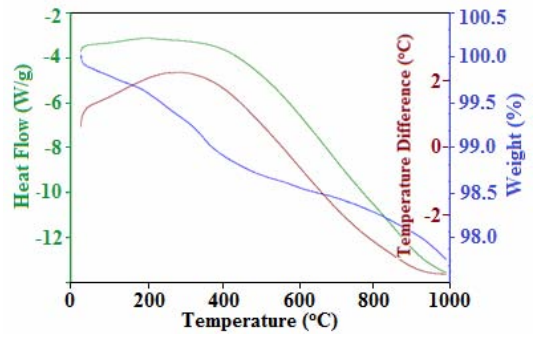

Fig. 3 — DTA/DSC-TGA traces of ZnY_2O_4

3.4 Energy Band Structures and Density of States Calculations

Figure 5(a-c) shows calculated electronic energy band structures, total DOS and PDOS of individual element O, Y and Zn in ZnY_2O_4. The Fermi level is pinned at 0 eV. Plane-wave basis set is generated with valence configurations of Y-[Ar]3d^{10}4s^{2}4p^{6}4d^{1}5s^2, O-1s^{2}2s^{2}2p^4, and Zn-[Ne]3s^{2}3p^{6}3d^{10}4s^2. Band in the range from ~–9.0 to 0.0 eV is the valence band (VB). Upper edge of the VB in the range from ~–5.5 to 0.0 eV is predominantly due to O 2p, Y 4s, 4p, 4d

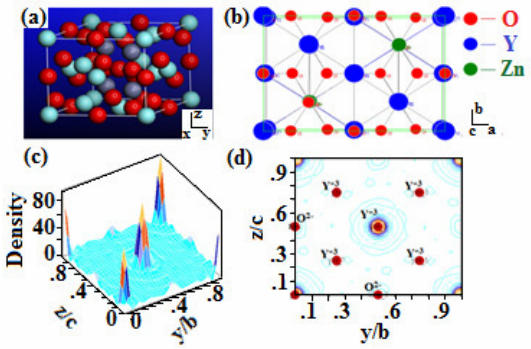

Fig. 4 — (a) Perspective view, (b) projection on to (001) plane of ZnY_2O_4, (c) 3-dimensional Fourier electron density along <100> plane and (d) electron density contour on (100) plane of unit cell structure of ZnY_2O_4

Table 2 — Position coordinates of the asymmetric unit of ZnY_2O_4

Sl. No.	Atom name	Crystal coordinates x	y	z	Cartesian coordinates before refinement x	y	z	Cartesian coordinates after refinement x	y	Z
1	Y1	0.0000	0.0000	0.0000	-5.4136	-3.7446	-3.0287	-5.4146	-3.7259	-3.0492
2	Y2	0.2500	0.7500	0.4000	-2.7068	1.8723	-0.6058	-2.7072	1.8629	-0.6099
3	Zn	0.2500	0.2500	0.2200	-2.7068	-1.8723	-1.6961	-2.7073	-1.8630	-1.7076
4	O1	0.2500	0.2500	0.4510	-2.7068	-1.8723	-0.2968	-2.7073	-1.8630	-0.2988
5	O2	0.0000	0.0000	0.5000	-5.4136	-3.7445	0.0000	-5.4145	-3.7259	0.0000
6	O3	0.1500	0.5000	0.3410	-3.7895	0.0000	-0.9631	-3.7902	0.0000	-0.9697

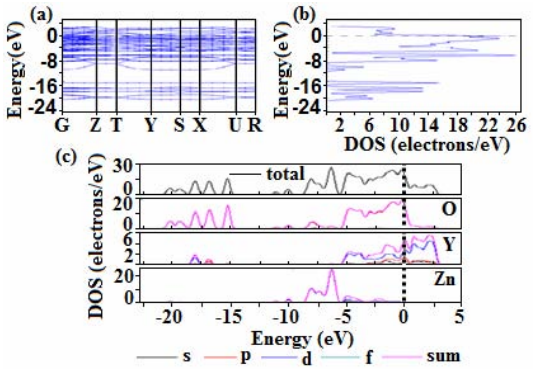

Fig. 5 — Calculated (a) electronic energy band structure, (b) density of states (DOS) and (c) partial density of states (PDOS) of elements O, Y and Zn in ZnY_2O_4

orbitals with very less contribution from Zn 3s, 3p, 3d orbitals. Lower edge of the VB in the range from ~–9.0 to –5.5 eV is mainly due to Zn 3d and O 2p orbitals. The core bands extend up to ~–21.0 eV. Since no high energy Zn orbitals are present above the Fermi level, the band gap narrows down significantly indicating the conduction band (CB), which is mainly formed from the contributions from Y 4s, 4p and 4d orbitals and spreads over the range from ~0.0 to 3.0 eV. As a result of smearing, the band gap, E_g, is observed to be ~0.011 eV. This result shows the very weak semicondcuting nature of ZnY_2O_4. This result also shows that the Zn-O bond mainly contributes to the formation of the VB while the CB is mainly formed from the Y-O bond in the crystal structure. Thus Zn-O bond has more of covalent character and Y-O bond has more of ionic character. Consequently, the charge-transfer band is expected and is indeed observed in the optical spectrum of ZnY_2O_4. Formation of O-Y-O or Zn-O-Zn bridges in the unit cell structure of ZnY_2O_4 is also evidenced from the powder XRD result of the sample.

3.5 Optical Absorption Studies

Figure 6 shows the optical absorption spectrum of ZnY_2O_4. The absorption band 200 nm in the UV region is assigned to the charge transfer (CT) transitions from oxygen 2p valence band to the Y 4d conduction band comprising the E_g orbitals[19] in octahedral splitting around $Y^{3+}(3d^{10}4s^24p^6)$ ion. The peak ~320–350 nm is due to O 2p→T_{2g} of Y^{3+} 4d orbitals in octahedral environment, and very weak peak ~600 nm is due to the d-d transitions in Y^{3+} ion in octahedral symmetry in the CB in the sample[19].

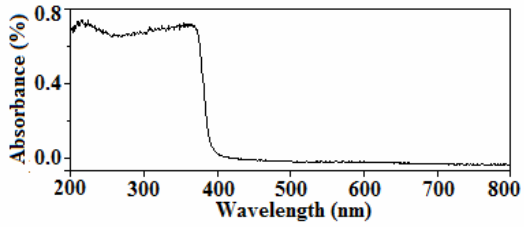

Fig. 6 — Optical absorption spectrum of ZnY_2O_4

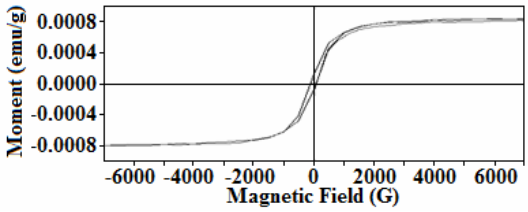

Fig. 7 — Magnetic moment versus magnetic field plot ZnY_2O_4 at 300 K

3.6 Magnetic Studies

Figure 7 shows the magnetic moment versus magnetic field plot of ZnY_2O_4 in the range from-7 kG to +7 kG. The presence of hysteresis loop clearly indicates the soft ferromagnetic nature of ZnY_2O_4 at 300 K. Fig.7 also shows the relatively low field saturation megnetization in ZnY_2O_4. The relatively low values of observed coercivity, 92.571 G, retentivity, 98.814×10^{-6} emu/g, magnetization 837.65×10^{-6} emu/g and magnetic susceptibility, 2.61×10^{-7} emu/gG show the soft ferromagnetic nature of ZnY_2O_4 at 300 K.

4 Conclusions

ZnY_2O_4 is synthesized by sol-gel method. Powder XRD result shows orthorhombic unit cell, space group Pccn and Z=4. Average crystallite size ~26-59 nm shows the formation of nanoparticles in the sample. Refinement of unit cell structure shows plausible lowering of the agreement factors with the lattice parameters: a=10.8290 Å; b=7.4518 Å; c=6.0985 Å. DFT calculation shows the energy band gap, Eg ~0.011 eV indicating weak semiconducting nature of ZnY_2O_4 oxide with CB predominantly formed from the Y valence orbitals. Magnetic moments data show weak ferromagnetic nature of the material at 300 K. Optical absorption result shows that the broad band around at ~320–350 and the very weak band ~600 nm are due to splitting of Y^{3+} ion 4d orbitals in octahedral symmetry in the conduction band (CB).

Acknowledgement

The authors thank Dr M M Balakrishnarajan, for help with the Materials Studio software.

References

1 Kaduk J A, Wong-Ng W, Greenwood W & Dillingham J, *J Res Nat Inst Stand Technol*, 104(2) (1999) 147.
2 Elilarassi R & Chandrasekaran G, *Opt Letts,* 6 (2010) 6.
3 Lincke H, Glaum R, Dittrich V & Tegel M, Z Anorg Allg Chem, 634 (2008) 1339.
4 Sarangi P P, Vadera S R, Patra M K & Ghosh N N, *Powder Technol*, 203 (2010) 348.
5 Brinker C J & Scherer G W, *J Non-Cryst Solids*, 70 (1985) 301.
6 Caruntu G, Bushb G G & O'Connor C J, *J Mater Chem*, 14 (2004) 2753.
7 Osaka T & Sayama J, *Electrochim Acta*, 52 (2007) 2884.
8 Epifani M, Melissano E, Pace G & Schioppa M J, *Eur Ceram Soc*, 27 (2007) 115.
9 Perdew J P, Burke K & Ernzerhof M, *Phys Rev Letts*, 77 (1996) 3865.
10 Segall M D, Lindan P L D, Probert M I J & Pickard C J *et al.*, *J Phys Cond Matt*, 14 (2002) 2717.
11 Clark S J, Segall M D, Pickard C J & Hasnip P J *et al.*, *Z Kristallogr*, 220(5-6) (2005) 567.
12 Hamman D R, Schlüter M & Chiang C, *Phys Rev Letts*, 43 (1979) 1494.
13 Popovic J, Grzeta B, Rakvin B & Tkalcec E *et al*., *J Alloys Compd*, 509 (34) (2011) 8487.
14 A.L. Patterson, *Phys Rev*, 56 (1939) 978.
15 McCusker L B, Dreele R B V, Cox D E & Louër D, *J Appl Cryst*, 32 (1999) 36.
16 Ono S, Brodholt J P & Price G D, *Phys Chem Miner*, 35 (2008) 381.
17 De Villiers P R & Herbstein F H, *Amer Mineral*, 53 (1968) 495.
18 Shannon R D, *Acta Cryst A*, 32 (1976) 751.
19 Krishnan S, Sandeep C S S, Philip R & Kalarikka N, *Chem Phys Letts*, 529 (2012) 59.